https://ntrs.nasa.gov/search.jsp?R=19790005816 2020-03-22T00:19:37+00:00Z

General Disclaimer

One or more of the Following Statements may affect this Document

- This document has been reproduced from the best copy furnished by the organizational source. It is being released in the interest of making available as much information as possible.

- This document may contain data, which exceeds the sheet parameters. It was furnished in this condition by the organizational source and is the best copy available.

- This document may contain tone-on-tone or color graphs, charts and/or pictures, which have been reproduced in black and white.

- This document is paginated as submitted by the original source.

- Portions of this document are not fully legible due to the historical nature of some of the material. However, it is the best reproduction available from the original submission.

Produced by the NASA Center for Aerospace Information (CASI)

NASA

Technical Memorandum **79677**

(NASA-TM-79677) AN INSTRUMENT TO MEASURE THE SPECTRUM OF COSMIC RAY IRON AND OTHER NUCLEI TO ABOVE 100 GeV-NUCLEON (NASA) 42 p HC A03/MF A01 CSCL 03B

N79-13987

Unclas
G3/93 40941

An Instrument to Measure the Spectrum of Cosmic Ray Iron and other Nuclei to above 100 GeV-Nucleon

J. F. Arens, V. K. Balasubrahmanyan,
J. F. Ormes, F. Siohan,
W. K. H. Schmidt, M. Simon,
and H. Spiegelhauer

November 1978

National Aeronautics and
Space Administration

Goddard Space Flight Center
Greenbelt, Maryland 20771

JAN 1979
RECEIVED
NASA STI FACILITY

AN INSTRUMENT TO MEASURE THE SPECTRUM OF COSMIC RAY IRON AND OTHER NUCLEI TO ABOVE 100 GeV/NUCLEON

J. F. Arens, V. K. Balasubrahmanyan, J. F. Ormes, F. Siohan*

NASA/Goddard Space Flight Center
Greenbelt, Maryland, U.S.A. 20771

W. K. H. Schmidt[/], M. Simon[+], H. Spiegelhauer

Max-Planck-Institut für Extraterrestrische Physik
Garching, W. Germany

*NAS/NRC Resident Research Associate

[/]Present address: Max-Planck-Institut für Aeronomie, Postfach 20, D-3411, Katlenburg, Lindau 3, W. Germany

[+]Present address: Gesamthochschule Siegen, 59 Siegen 21, Physics Department, W. Germany

ABSTRACT

A balloon-borne detector system for extending the study of cosmic ray composition to the energy region beyond 100 GeV/nucleon is described. The geometry factor of the instrument is 0.64 m^2sr and in a successful flight data was collected for 27 hours at 6-7 g/cm^2 altitude The instrument incorporates an ionization calorimeter and a gas Cherenkov counter filled with freon 12 to 20 P.S.I. (ref. index 1.0014) for determination of energies and a charge module consisting of scintillation and a lucite Cherenkov counter for determination of the charge of the incoming particle. The scintillators were utilized to determine the position of the incoming particle in addition to its charge. The characteristics of these detectors with respect to resolution, and the methods employed in laboratory calibration, cross-checks with flight data and actual performance in the flights are described in detail. The response of a calorimeter to complex nuclei, until now has been extrapolated from the calibration with protons at accelerators. Monte Carlo simulation of the ionization calorimeter and comparison of the response of the calorimeter and gas Cherenkov counter for complex nuclei have enabled us to convert the observed calorimeter signal to absolute energy in a consistent manner. The limitations of the present detector system and suggested future improvements are discussed.

1. Introduction

In the past few years it has become evident that the nuclear composition of the cosmic radiation is energy dependent These observations have generated a very lively discussion concerning the current picture of cosmic ray confinement, propagation and origin (Ormes and Freier, 1978, Orth et al., 1978, Caldwell, 1977, Simon, 1977, Lezniak et al 1977). The data available at present range roughly up to 100 GeV/nucleon and they were mainly obtained by employing ionization spectrometers, gas Cherenkov counters or magnetic spectrometers. For extending the measurements beyond 100 GeV/nucleon one has to meet two major requirements with any balloon-borne instrument:

It must have a large geometric factor and the capability of covering a large dynamic range in charge and energy. Here an instrument will be described which extended the measurements beyond 100 GeV/nucleon and which combined an ionization spectrometer and a gas Cherenkov counter for performing two independent energy measurements. The combination of these two systems provided for the first time an experimental cross-check on the response of both types of detectors. It was possible to test the spectrometer response for heavy nuclei by means of the gas Cherenkov response curve and vice versa to study the properties of the Cherenkov detector residual scintillation light by means of the spectrometer response.

The charge of the incident particle was measured by a combination of scintillators and an acrylic Cherenkov counter and the trajectories of the incident particles were determined by position sensing scintillators (Schmidt and Simon, 1975, Scarlett et al., 1975, Arens, 1974). This

technique was chosen in order to avoid a pressurized gondola for the large size of this experiment.

The experiment was launched on October 11, 1976 and successfully flown at an altitude of 6-7 g/cm^2 for 27 hours, thus providing an exposure of 16 m^2 sr hr. The total suspended payload was 3450 kg which represents an upper limit for the size and weight that can practically be launched using the dynamic technique commonly employed.

The characteristics of this instrument will be presented in detail in the following chapters. The results and their astrophysical implications will be presented in a future paper.

2. The Apparatus

Figure 1 shows a schematic cross section drawing of the balloon-borne cosmic ray experiment. The whole instrument consisted basically of three major components:

(1) A Gas Cherenkov counter on top of the instrument for determining the charge and velocity of the incoming particles.

(2) The Charge Measuring Module which consisted of five scintillators and a solid Cherenkov counter. The scintillators were also used as entopistic, i.e. position sensing systems by utilizing the non-uniformity of scintillation light collection to determine the traversal position of each particle.

(3) An Ionization Spectrometer or calorimeter for determining the energy of the incident particle. This spectrometer consisted of a sandwich containing iron plates and plastic scintillator layers divided into three modules.

Since a pressurized gondola was precluded by the large size of the instrument, each phototube had its own potted high voltage supply. For the balloon flight, the instrument was placed in a styrofoam housing for purposes of thermal insulation. The weight of the scientific payload was 2653.6 kg.

The sensitive area of the apparatus as defined by the upper scintillator was 1.2 m x 1.2 m and the geometric depth was 1.0 m. This provided a geometric factor of 0.64 m^2 sr, which reduced to 0.32 m^2 sr for those particles which penetrated both the gas Cherenkov counter and the spectrometer. the experiment could operate in 4 modes: The principal flight mode was a threshold condition of 12 times the minimum ionizing pulse height in the scintillators S1x, S1y, S3x and S3y as defined in Figure 1. A more stringent mode had an additional condition that the third iron module have a signal of 18 minimum ionizing particles. Another mode accepted protons and was enabled every fourth event. For calibration purposes there was a "wide open" mode which was enabled every thirty-second event.

3. Position Detection

The configuration of the detectors which measured the charge and determined the traversal positions is illustrated schematically in Figure 2. All scintillators were made of Pilot Y material. The solid Cherenkov detector had a 1 cm thick radiator with a waveshifter which reemits U.V. radiation at 425 n.m. (Pilot 425). The scintillators labeled S1x and S1y both had a thickness of 0.64 cm, while S2 was 1 cm thick, S3x was 0.64 cm, S3y was 1.0 cm, and S4 was 2.0 cm. The

gas counter was made of 0.5 cm thick aluminum and the top and bottom plates were curved as shown in Figure 1 to minimize path length compensations, while maximizing their pressure carrying capability. The counter was filled with Freon 12 to a pressure of 20 psi (n = 1.0014), providing a threshold energy of 16.5 GeV/nucleon. All the detectors were viewed edge-on through acrylic light pipes which were optically coupled to the scintillators, or white diffusion boxes as indicated in Figure 2. The diffusion boxes were painted with a special high reflectivity paint (Schutt et al. 1974).

Each phototube (RCA 4525 and RCA 4524) was pulse height analyzed separately except for the tubes on S4 and on the two Cherenkov counters. The two tubes on each edge in S4 were summed before pulse height analysis. The light diffusion tent of the solid Cherenkov counter was viewed by 8 phototubes from which the odd and the even numbered ones (proceeding clockwise around the diffusion box) were separately summed and pulse height analyzed, thus minimizing the non-uniformity of light collection. The gas Cherenkov counter had six phototubes also divided into two sets and separately summed and pulse height analyzed. The lucite windows through which the gas Cherenkov radiation was viewed were coated with β-terphynyl for shifting the U.V. light to match the spectral response of the P.M. tubes. In order to accomodate the dynamic range required for the different detectors, the signals were analyzed simultaneously from both the fifth and tenth dynodes of the individual phototubes.

In the center of the different scintillators we measured 70 to 140 photoelectrons, depending on the scintillator, and in the solid Cherenkov

counter about 10 photoelectrons, for relativistic muons of vertical incidence The gas counter provided roughly 130 photoelectrons for oxygen nuclei at energies exceeding 100 GeV/nucleon (plateau value).

The two sets of PMT's viewing the solid Cherenkov detector and the four scintillators S1x, S1y, S3x and S3y provide six independent measurements of charge, but due to their large dimensions and to large accepted angles of incidence, corrections had to be applied to the raw pulse heights. These corrections had to account for variations of the detector response over its sensitive area and for the zenith angle dependence of the path lengths in the scintillators.

For the trajectory measurement, the position of incidence was located by utilizing the non-uniformity of scintillation light collection. Arens (1974), Schmidt and Simon (1975), Scarlett et al. (1975) have recently reported development work on such an approach. The basic idea is that the measured signal of a penetrating particle depends on its distance and location in the scintillator relative to the phototubes.

A ratio function

$$f(x,y) = A/(A+B) \qquad (1)$$

was constructed from the pulse heights of two phototubes A and B which served to determine a locus of points in a scintillator layer. By two such measurements in perpendicular directions a complete localization could be achieved. Actual pulse height measurements are of course subject to errors, so that in reality only a strip of finite width can be determined. The minimum width of this strip is given by the uncertainty of f due to photoelectron fluctuations. The standard deviation at a certain position (x,y) is

$$\frac{\Delta f\ (x,y)}{f\ (x,y)} = (1-f(x,y))\ \left(\frac{1}{N_A(x,y)} + \frac{1}{N_B(x,y)}\right)^{\frac{1}{2}} \qquad (2)$$

where $N_A(x,y)$ and $N_B(x,y)$ are the number of photoelectrons at the the position (x,y) as measured by the phototubes A and B, respectively. Since the light production in the scintillators is approximately proportional to Z^2, the standard deviation ($\Delta f/f$) is inversely proportional to the charge of the incident particle favoring this technique for heavy cosmic ray nuclei. The spatial resolution which is finally obtained is limited by the photoelectron statistics (equation 2) and by the gradient of the ratio function f at a particular position.

The function f has the advantage of being independent of the charge, the velocity, the angle of incidence and Landau fluctuations of the individual event. The function f is not even influenced by interactions of the incident particle. These effects all cancel out, since we take the ratio of A and A+B.

To obtain the pattern of f-values in the scintillation detectors, a pulsed ultraviolet light source was used to simulate the passage of charged particles. To avoid any contamination with visible light, which might be refracted by surface scratches into directions of total internal reflection, we used a filter with a 100 Å transmission band centered at 3600 Å. The spectrum of light emitted through the filter and the light transmission curve through the scintillator are shown in Figure 3. As can be seen, the ultraviolet light is absorbed by the scintillator and reemitted as isotropic light of longer wave length, just as when a particle

traverses the detector. The isotropization was experimentally confirmed by varying the angle of incidence of the collimated ultraviolet light at one end of a long scintillator. This test yielded signals constant to at least 5% in a phototube at the other end of the scintillator. A further check on the isotropy of scintillation light was performed by comparing the response for cosmic ray muons with that for the light source. Results obtained using an ultraviolet source on the one hand and charged particles on the other might be expected to show some differences because of surface effects, propagation effects in the scintillators or because of differences in the emitted light spectra. We found that the ratio of phototube pulse heights made with ultra-violet light and with muons agreed to about 1%.

A scanner was built to carry the ultraviolet light source automatically to a grid of points over the scintillator to be mapped. The light was vertically incident on the scintillators. Typically, 400 light pulses were flashed at each of the positions, which were 2 to 5 inches apart, depending on the scintillator. The phototube responses were pulse height analyzed and stored on magnetic tape for further analysis. Each scintillator could be mapped within a few hours.

Two principal types of position determining detector systems were used in this experiment. The first type (S1 and S3, see Fig. 2) contained a pair of scintillators viewed by 2 tubes each, thus yielding two "orthogonal" coordinates and a complete localization. The second type (S2 and S4) was viewed by four tubes or tube groups which gave a position determination by a single scintillator. As an example Figure 4 shows the ratio contour

lines in S1. The position of a flight event was found simply by searching the area for the grid point where the two flight data ratios were closest to the map ratios in terms of the ratio variances. The ratio variances were determined in the ultraviolet mapping. The positions in S2 and S4 were found by using the four ratios, A/(A+C), B/(B+D), (A+B)/(A+B+C+D) and (B+C)/(A+B+C+D) as given in Figure 2.

Table I lists the spatial resolution obtained in the center of the different detectors. These numbers refer to oxygen nuclei, but only a weak dependence on the charge could be found, indicating that systematic uncertainties determined the ultimate resolution and not photo electron statistics.

The particle trajectories were computed as least square lines through the penetration positions in the different scintillators. Figure 5 shows the number distribution of cosmic ray particles accepted by the instrument versus the cosine of the zenith angle ϕ. The curve depicts the theoretical distribution to be expected for the given geometry of the instrument under isotropic irradiation, which compares well with the measurements. In Figure 6 are shown the location of trajectories at the level of the gas Cherenkov detector selected for events which gave both large and roughly consistent (within a factor of 2) pulse heights from the two sets of gas counter PMT's. No other selection criterion has been applied.
These events all have greater than 32 GeV/amu energy deposit in the calorimeter. It can be seen that only a few events lie outside the expected area. Comparable spatial distributions have been made to check that particles

which give large pulse heights in the bottom iron module do in fact have trajectories which traverse the bottom of the counter rather than exiting through the side.

All these figures demonstrate good agreement between the measured distributions and those distributions expected on the grounds of theoretical considerations. This gives us confidence that, for events with well defined charges, the trajectories determined by this technique provide an adequate description of the particles' paths through the instrument.

On the basis of our experience with this position determining scintillator system we can list its characteristics as follows:

(a) The large area scintillators provide the modest resolution required.

(b) The need for a pressure housing for gas filled proportional counters or spark chambers is eliminated.

(c) The signals from the same detector can be used to determine the charge and the location of the incident particles.

(d) The scintillators are relatively rugged devices, and reasonably priced.

(e) Position measurements are insensitive to ionization loss fluctuations due to delta-electrons accompanying the heavier particles.

(f) The system is susceptible to background from multiple particle events.

(g) Background may mimic the wrong trajectories.

(h) The scintillators must be carefully mapped and the gain drift of each photomultiplier must be carefully monitored.

We believe, however, that the accuracy of the trajectory determination which was obtained in this flight is not the ultimate limit of the technique. Tailoring the scintillators to create an orthonormal set of isolumes with a larger intensity gradient would greatly improve the resolution. An easy in-flight calibration of the gain of each should also improve the accuracy. This could be done using inflight particles simply by employing a small scintillator telescope within the telescope geometry. Any type of particle passing through this area provides a calibration of the phototubes and would also indicate phototube gain drifts. Alternatively, a light-emitting diode optically coupled to each scintillator could also provide in-flight monitoring. The problems of multiple incident particles and background events will be discussed in detail in a separate paper.

4. Charge Determination

The charge was determined from the five charge detectors (S1x, S1y, S3x, S3y, solid Cherenkov counter) using a multi-detector maximum-likelihood technique and the background was estimated by examining the resulting χ^2-distribution. Corrections for the spatial non-uniformity of the scintillators were determined from the flight data. Carbon and oxygen nuclei were used to adjust the amplitude maps made prior to flight with the u.v. lamp. Good events were selected based upon the charge analysis χ^2 values and mean pulses were found in an array of 5x5 cells on each detector. Mean pulses were corrected to better than 1%. The charge resolution is probably limited by the uncertainty in the trajectory and position of the particle in the scintillator.

In this experiment it turned out to be important to study the individual dependence of signals in the different detectors on charge and energy. It was observed that the average charge signal in each detector showed an increase with energy. In Figure 7, the enhancement of the average charge signals as a function of energy is shown as derived using oxygen nuclei. A worsening was also seen in the charge resolution with increasing energy. The figure illustrates that the enhancement of the average signal is more pronounced the closer the detector is situated to the spectrometer and the high the energy. It is also observed that the S_3 signals are consistently lower for those particles which have not interacted in the first iron module (Fe 1) than for those which have significant cascading. The curves in Figure 7 can be thought of as representing the most probable energy deposit for particles interacting in Fe 1 and as the average energy deposit for those interacting deeper down. No attempt has been made to adjust for this effect because the fluctuations in energy loss are quite large for heavier particles. The affected detectors (S3x and S3y) are excluded from the analysis for heavy nuclei. They are considered for carbon and oxygen nuclei to aid in understanding the effects of background at high energies. We attribute this behavior in large part to an energy dependent amount of back flowing energy in the form of particles from the iron spectrometer. The effect is less pronounced in S1x, S1y and the solid Cherenkov counter since these detectors are further away from the spectrometer and additionally shielded by S2, S3x and S3y. The enhancement in the detectors S1x, S1y and solid Cherenkov counter is quantitatively consistent with being casued by

δ-ray production between 1 and 20 GeV/nucleon (Yodh, 1977).

Figure 8 shows the charge resolution achieved for particles exceeding the geomagnetic cut off of 1.5 GeV/nucleon at Palestine (Texas). For this sample of particles a charge resolution was 0.3 charge units for oxygen and about 1.3 charge units around iron.

In this energy region the charge resolution is limited by the uncertainties with which the trajectories could be measured. At higher energies the charge resolution becomes worse and is determined by background effects.

5. The Ionization Spectrometer

The ionization spectrometer was the principal detector for determining the energy of cosmic ray nuclei. The primary particle converts a great part of its initial kinetic energy into a nuclear electromagnetic cascade which builds up by a series of nuclear interactions in the spectrometer. The ionization dissipated by the cascade is then measured by sampling the ionization energy loss at various depths in the absorber. In this experiment the iron slab and scintillator sandwich used was divided into three modules. Each module contained two scintillators and was viewed from two opposing sides by phototubes at the ends of white light guides, as shown schematically in Figure 9. A vertically incident cosmic ray encounters a total of 170 g/cm^2 iron plus 5.9 g/cm^2 scintillator material, which corresponds to 1.44 proton and approximately 6 iron nuclear interaction lengths. The response and the characteristics of this spectrometer were deduced from Monte Carlo simulations (Jones et al., 1977) and experience obtained from similar spectrometers flown in earlier flights (Schmidt et al., 1976; Balasubrahmanyan and Ormes, 1973). For the energy deter-

mination the sum of the signals from the three modules with corrections made for the location of the first interaction was used. Figure 10 shows a pulse height distribution of the sum of signals for carbon nuclei of 100 GeV/nucleon as deduced from the Monte Carlo simulation. The pulse height in this case is expressed in equivalent muons per nucleon, the signals are given in units of the mean energy loss of vertically incident minimum ionizing muons. The large peak at low signals represents those events which go through without any interaction.

The cross hatch histogram is selected for events which "interacted" in the first iron module. The selection was based upon signal indicating a response 25% greater than that for a minimum ionizing carbon nucleus or the equivalent of 3.7 particles per incident nucleon. For this selected subset of 164 Monte Carlo generated events, the resolution was 30% whereas for the whole sample it was closer to 60%.

Table II gives the expected response of the calorimeter for vertically incident nuclei. The standard deviation does not give an accurate idea of the expected resolution of the calorimeter because of the large fraction of noninteracting events contributing to the width of the signal distribution. and due to the fact that the calorimeter signal increases more slowly than energy ($E \sim S^{1.3}$). Also the incident cosmic ray spectra are steep ($dN/dE = AE^{-\gamma}$ with $\gamma \sim 2.5$) and so in the cosmic ray beam higher energy particles are less abundant.

With primary integral energy exponents -1.4, -1.5, & -1.6, for carbon, silicon and iron nuclei Monte Carlo calculations at 6, 17.6, 30 and 100 GeV/nucleon were weighted for the spectral distributions. The energy

E' for each of these energy bins at 6, 17.6, 30, and 100 GeV/nuc was picked at random from an exponential distribution weighted for the incident spectrum. The signal S' corresponding to the selected energy E' was found to be

$$S' = (E'/E)^{1/\alpha} S \qquad (3)$$

where $\alpha \simeq 1.2$.

In dealing with cosmic ray energy spectra one has to consider that a measured spectrometer signal is most probably caused by an energy which is smaller than that given by the formula above. This is due to the limited spectrometer energy resolution and to the steep cosmic ray spectrum. Figure 11 shows the probability that a carbon nucleus of energy E produces a signal of 200 equivalent muons per nucleon in the spectrometer assuming a carbon energy spectrum with an integral slope of -1.6. According to formula (3) which represents the mean response of the calorimeter, 200 equivalent muons refer to 143 GeV/nucleon, whereas according to Figure 11, 200 equivalent muons are most probably produced by cosmic ray carbon nuclei of about 80 GeV/nucleon. It is worth noting that no particle below 40 GeV/nucleon can produce a signal of 200 equivalent muons per nucleon in the spectrometer. The long tail to higher energies in Figure 11 is made by those particles which have not yet developed a reasonable cascade in the spectrometer.

6. The Gas Cherenkov Counter

For the first time a gas Cherenkov counter and an ionization spectrometer have both been flown in a high energy cosmic ray experiment. This offers a unique advantage in three respects:

1. The gas Cherenkov counter pulse height response distribution can be studied in terms of the residual scintillation light and the Cherenkov light
2. The gas Cherenkov counter response provides an in-flight calibration of the ionization spectrometer.
3. The energy spectra of the cosmic ray nuclei can be determined by a deconvolution of the observed gas Cherenkov counter response and independently by the ionization spectrometer providing a cross-check between these two techniques which have been separately used in previous high energy cosmic ray experiments.

Usually the gas Cherenkov response distributation is contaminated by residual scintillation light. The exact amount of this contribution and the shape of its distribution is crucial in order to deconvolute properly the cosmic ray spectrum, (Juliusson, 1974, Lezniak 1975). In this experiment, it was possible to study the gas Cherenkov response distribution in different energy regimes since the ionization spectrometer provided an independent energy determination. This enabled us to separate scintillation light from Cherenkov light. Figure 12 shows the overall signal response distribution of the gas counter as measured for oxygen of energies greater than 12 GeV/nucleon. There are two pulse height regions visible. The peak at low pulse heights consists of particles producing pure scintillation light which was found to be Z^2 dependent. The greater pulse height signals are caused by the Cherenkov light of oxygen nuclei exceeding the threshold energy of 16 GeV/nucleon.

The energy cut at 12 GeV/nucleon was chosen in order to have both phenomena on one graph. If the spectrum were cut at lower energy, the scintillation light would totally dominate. It is evident from Figure 12 that the tail of the scintillation light distribution extends into regions of higher pulse heights. The shape of this tail can, however, be deduced from a figure in which one plots the counter response distribution for energies below 12 GeV/nucleon. These particles then produce only scintillation light. This has been done and the dotted curve in Figure 12 represents the shape of this distribution. Thus, we are able to take into account the amount of the residual scintillation light in the gas Cherenkov counter in the deconvolution procedure.

The gas Cherenkov counter in turn permits us to check the ionization spectrometer response function, which has been deduced by Monte Carlo simulation (see section 4). A comparison of the gas Cherenkov response and the ionization spectrometer response is shown in Figure 13. Oxygen nuclei were selected which have deposited at least 5 GeV/nucleon in the spectrometer and which have trajectories exiting through the bottom. Checks indicate that the Monte Carlo simulations and the gas Cherenkov response agree for all nuclei carbon through iron in the energy range 16 GeV/nucleon to 100 GeV/nucleon. The curve drawn in this graph represents the theoretically expected gas Cherenkov response. The calculation of this curve has been done under the following four assumptions:

1. The index of refraction of the gas (Freon 12 at 20 psi) was $n = 1.0014$.
2. The residual scintillation light is 4 channels on this plot.

3. The integral energy spectrum of the cosmic ray oxygen nuclei was assumed to have a slope of -1.6.
4. The energy scale in Figure 13 is expressed in equivalent muons per nucleon and the energy used in the gas Cherenkov response calculation is the most probable energy as explained in section 5.
5. The saturation level of the Cherenkov signal was chosen as the only free parameter in the calculation of the Cherenkov response curve.

From the good overall agreement between the curve and distribution of dots and the correct position of the threshold we have a fairly good check on the interpretation of the spectrometer response.

Once the response as a function of energy is known, the asymptotic response of the gas Cherenkov detector at high energy (>100 GeV/amu) can be computed for all the charges, or equivalently, a given gas Cherenkov response can be used to determine the charge. A comparison of this charge can be made with the charge determined by the χ^2 analysis of the S1x and S1y scintillators and the solid Cherenkov. Such a comparison is shown in Figure 14. In the charge range above Si, the gas Cherenkov detector saturated due to an electronic malfunction. This meant that the asymptotic response for iron nuclei could not be checked. However, high energy particles (>30 GeV/nucleon) were "tagged" by the gas Cherenkov for all charges.

Summary

A large area detector system was flown on a balloon utilizing both a calorimeter or ionization spectrometer and a gas Cherenkov detector for measuring energy. The resultant inflight calibration of the calorimeter removes the one remaining uncertainty in the use of ionization calorimeters for heavy nuclei, namely the absolute energy scale. Previously all studies of calorimeter response were done for protons only at high energies (e.g. Fermilab studies up to 400 GeV) and for heavy nuclei only at 2.1 GeV/nucleon (Bevelac studies using heavy nuclei). At low energies (< 10 GeV/nucleon) the effects of ionization energy loss and nuclear fragmentation are important. Our calibration indicates that those effects have been understood and correctly accounted for in the Monte Carlo simulations, and that the response of the calorimeter for high energy heavy nuclei is well understood. It should be remarked that this statement holds even though the calorimeter is only 1.44 interaction lengths deep.

Also the effect of the shape of the distribution of the residual scintillation light on gas Cherenkov detectors has been studied. Such an effect could tend to steepen an observed spectrum if not properly taken into account.

Spatial resolution of 5-10 cm was obtained using the ratios of pulse heights in different photomultiplier tubes looking at the same scintillators. This technique is ideally suited for making position measurements in large area detector arrays. Its chief disadvantage lies in its susceptibility to background induced by large air showers in which N particles simulate a particle of charge $Z = N^{\frac{1}{2}}$. Many such events can be eliminatd by requiring consistency between the response of all the scintillators, but in the continuum of possibilities, a significant background still exists for

the lower charged particles which would be easily removed by a more explicit "picture" device.

The properties of energy backflowing from the calorimeter have been studied and suggest that segmenting the scintillators directly above the calorimeter or shielding them using lower Z material would be useful for energy above 50 GeV/amu. Between 1 and 20 GeV/nucleon, the increase in signal due to the increasing probability of producing penetrating delta rays is observed.

This paper has focused on the details of the experiment and its response to heavy cosmic ray nuclei. The spectra derived therefrom and the astrophysical interpretations of those spectra will be presented elsewhere. This balloon borne payload was the heaviest (3467 kg suspended) cosmic ray experiment every flown above 30 km, and represents the limit of what should be attempted using the dynamic launching technique commonly employed.

Acknowledgement

We would like to thank Dr. W. V. Jones for the use of his Monte Carlo simulations of the nuclear electromagnetic cascades in the calorimeter and Dr. G. B. Yodh for his calculations of the signal to be expected from the delta ray contributions at higher energies. Mr. C. R. Greer, Mr. G. Cooper and Mr. A. Puig helped build and test the detectors and carried out the field support of the experiment. Mr. J. Laws provided the able electrical engineering support. The NSBF provided the launch and balloon operations support. Without the effort of each of the persons involved the experiment could not have been done. The support and encouragement of F. B. McDonald and K. Pinkau is grealy appreciated. This experiment was also supported by the Bundesminister fur Forschung und Technologie of the Federal Republic of Germany under the title WRK244 and WRK0275:5.

TABLE I

MEASURED SPATIAL RESOLUTION OBTAINED FROM OXYGEN NUCLEI IN THE CENTER OF THE DIFFERENT DETECTORS.

DETECTOR	S1x	S1y	S2	S3x	S3y	S4
Spatial Resolution (cm)	5	5	10	5	7	15

TABLE II

RESOLUTION OF THE SPECTROMETER AS DEDUCED FROM MONTE CARLO SIMULATIONS

Energy (GeV/nucleon)	6	17.6	30	100
C $\frac{\sigma}{\mu}$	34%	45%	50%	58%
Si $\frac{\sigma}{\mu}$	18%	32%	39%	49%
Fe $\frac{\sigma}{\mu}$	11%	26%	35%	46%

References

Arens, J. F., Nuclear Instruments and Methods, 120, 275 (1974)

Schutt, J. B., Arens, J. F., Shai, C. M., Stromberg, F., Applied Optics 13, 2218 (1974)

Jones, W. V., Physical Review, 187, 1868 (1969)

Juliusson, E., Ap. J., 191, 331 (1974)

Lezniak, J. A., Webber, W. R., Kish, J. C., Simpson, G. A., 15th Intl. Cosmic Ray Conf., Plovdiv, Vol. 1, 237 (1977)

Lezniak, J. A., Nucl. Inst. and Meth. 126, 129 (1975)

Ormes, J. F., Frier, P. S., Ap. J. 222, 471 (1978)

Scarlett, W. R., Frier, P. S., Waddington, C. J., preprint 14th Intl. Cosmic Ray Conf., Munich, 3, 161 (1975)

Schmidt, W. K. H., Simon, M., Nucl. Inst. and Meth. 123, 333 (1975)

Simon, M., Astron. and Astrophys. 61, 833 (1977)

Jones, W. V., Ormes, J. F., Schmidt, W. K. H., Nucl. Inst. and Meth. 140, 557, (1977)

Balasubrahmanyan, V. K. and Ormes, J. F., Ap. J. 186, 109 (1973)

Schmidt, W. K. H., Atallah, K. A., Cleghorn, T. F., Jones, W. V., Modlinger, A., Simon, M., Astron. and Astrophysics 46, 49 (1976)

Caldwell, J. H., Ap. J. 218, 269 (1977)

Orth, C. D., Buffington, A., and Smoot, G., preprint, L.B.L.-7553, Lawrence Radiation Laboratory (1978)

Yodh, G. B., private communication, (1977)

Figure Captions

Figure 1. Schematic diagram of the balloon-borne instrument.

Figure 2. Configuration of charge and position measuring detectors and arrangement of photo-tubes (not to scale).

Figure 3. The spectrum of light through the U.V. filter used for calibration and the spectral response of the scintillator. The U.V. light is shifted down in wavelength and emitted isotropically in the scintillator.

Figure 4. The ratio map of scintillator S1 obtained by the U.V. light calibration in the laboratory.

Figure 5. Angular distribution of cosmic ray particles detected in flight. The curve is a Monte Carlo simulation for isotropic radiation incident on the instrument.

Figure 6. The location of trajectories of particles at the gas Cherenkov counter for the case when the particles gave consistent and large pulse heights from the two sets of P.M. tubes.

Figure 7. The signals in various detectors as a function of energy. The increase in S1X, S1Y and $\overset{v}{C}_e$ and $\overset{v}{C}_o$ are consistent with a contribution of energy deposit due to increase of knock-on probability with energy. The case of the S3X scintillator is different from S1X, S1Y, $\overset{v}{C}$ and $\overset{v}{C}o$ and is suggestive of back-flow of energy from the ionization spectrometer.

Figure 8. Charge distribution for particles of energy > 1.5 GeV/nucleon at Palestine, Texas. The charge resolution was 0.3 charge units for oxygen nuclei and increases to 1.3 charge units around iron.

Figure 9. Schematic diagram of the ionization spectrometer.

Figure 10. Monte Carlo simulation for carbon nuclei incident on the ionization spectrometer. The large peak at low signals is due to particles which do not interact in the spectrometer.

Figure 11. Probability for a carbon nucleus at different energies with an assumed power law spectrum ($\gamma = -1.6$) to produce a signal of 200 equivalent muons/nucleon. Notice that the long tail towards higher energies is due to particles which have not interacted in the spectrometer.

Figure 12. Pulse height distribution for oxygen nuclei for energies $>$ 12 GeV/nucleon. The dotted curve is the contribution of ionization loss in Freon 12, obtained from the study of particles below the gas Cherenkov threshold.

Figure 13. Comparison of the ionization spectrometer response and gas Cherenkov counter response for oxygen nuclei. Similar agreement is seen for all other nuclei.

Figure 14. Comparison of the charge obtained from the charge module (S1X, S1Y, and solid Cherenkov) and the charge as obtained by the gas Cherenkov counter for particles with energy $>$ 64 GeV/nucleon.

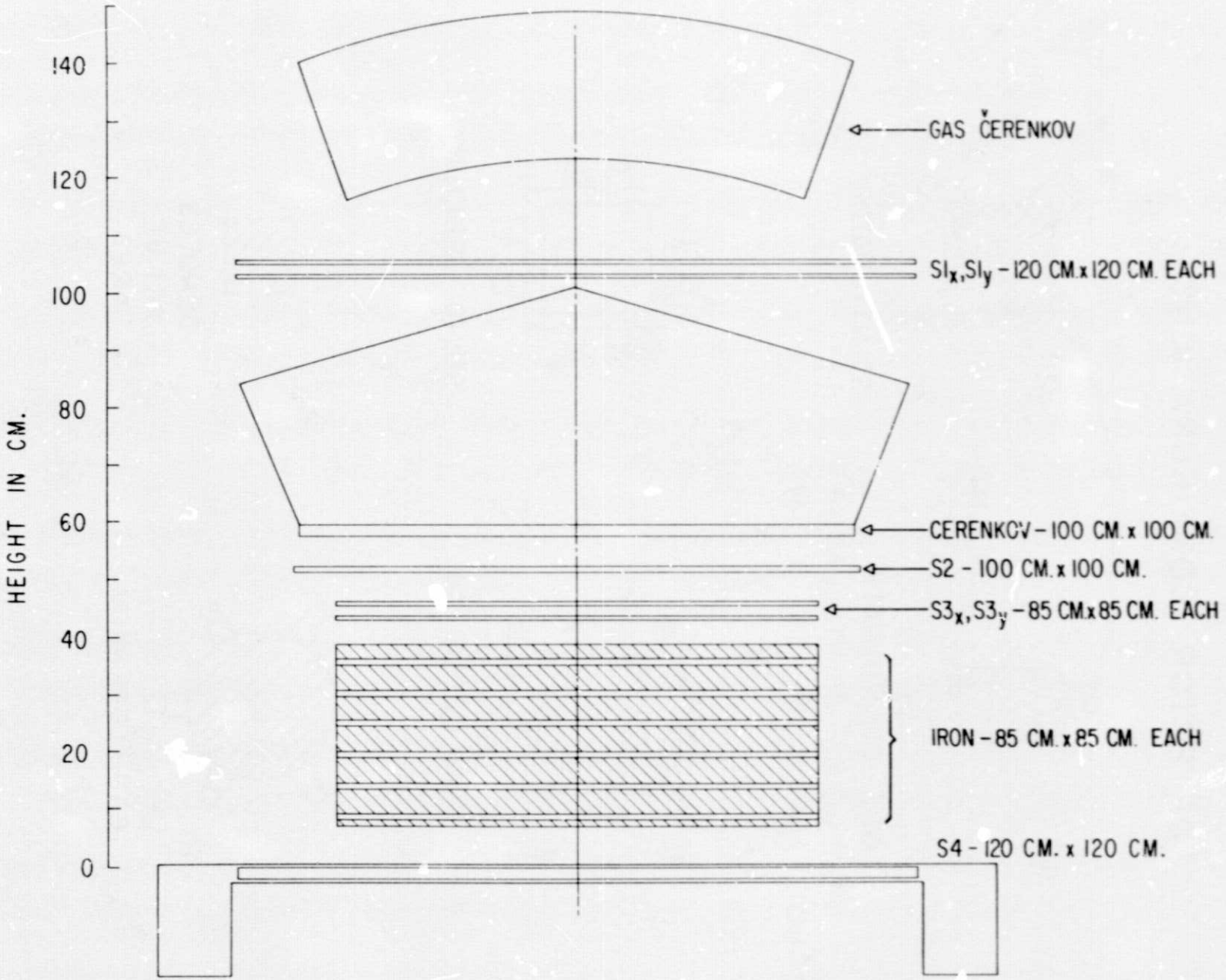

GERMAN-AMERICAN HIGH ENERGY COSMIC RAY TELESCOPE

DETECTOR CONFIGURATIONS

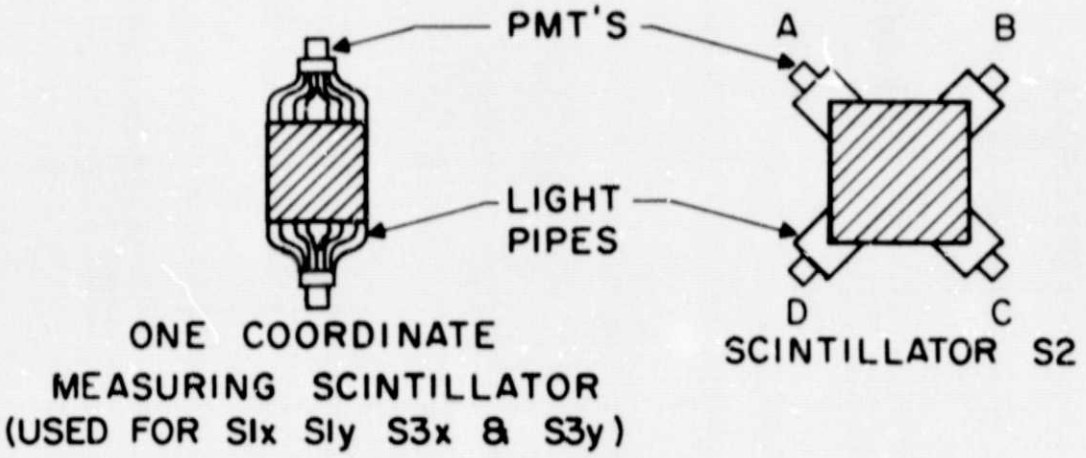

ONE COORDINATE MEASURING SCINTILLATOR (USED FOR S1x S1y S3x & S3y)

SCINTILLATOR S2

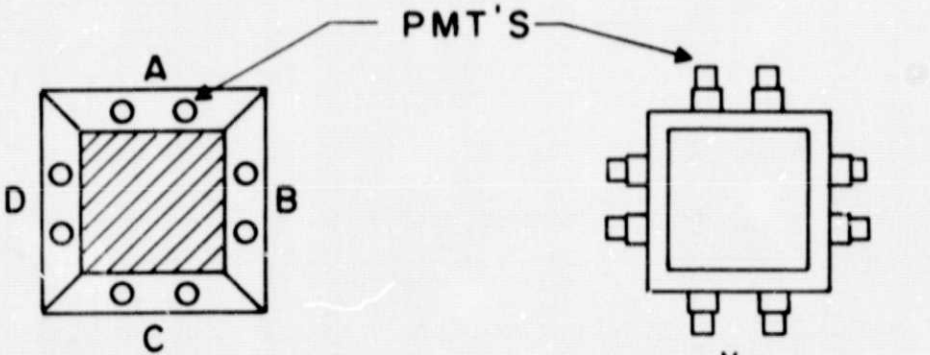

SCINTILLATOR S4

SOLID ČERENKOV

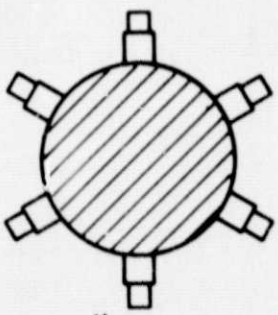

GAS ČERENKOV

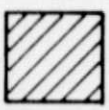

DENOTES ACTIVE AREA

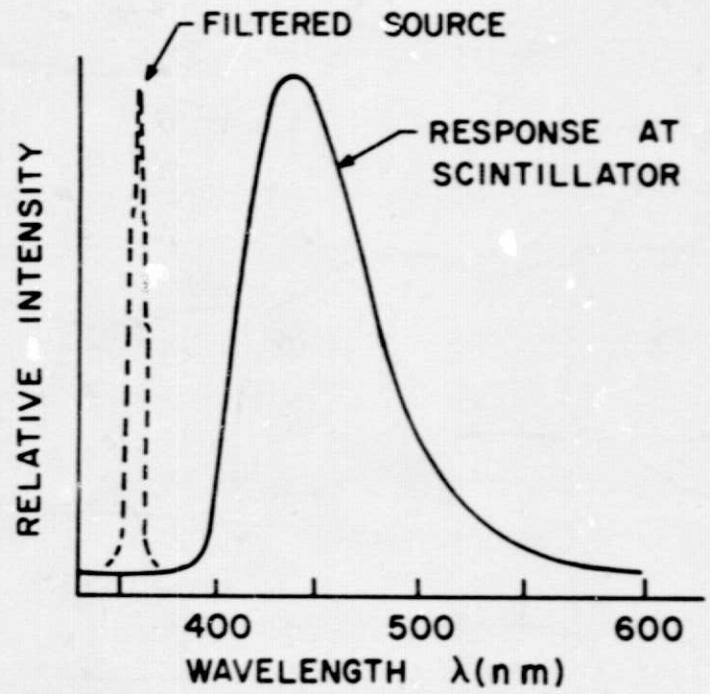
FILTERED SOURCE
RESPONSE AT SCINTILLATOR
RELATIVE INTENSITY
400
500
600
WAVELENGTH λ(nm)

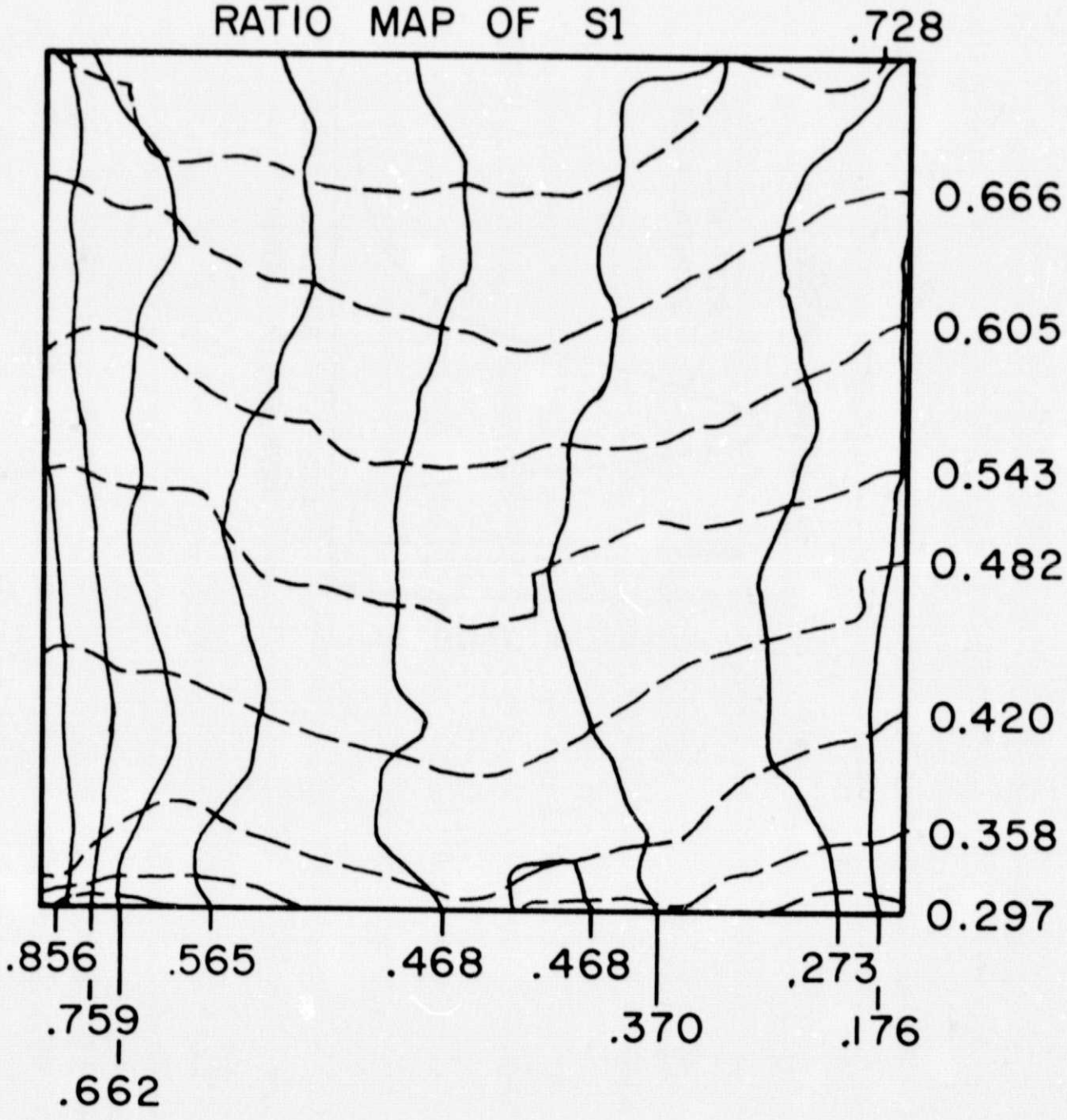
RATIO MAP OF S1
.728
0.666
0.605
0.543
0.482
0.420
0.358
0.297
.856
.759
.662
.565
.468
.468
.370
.273
.176

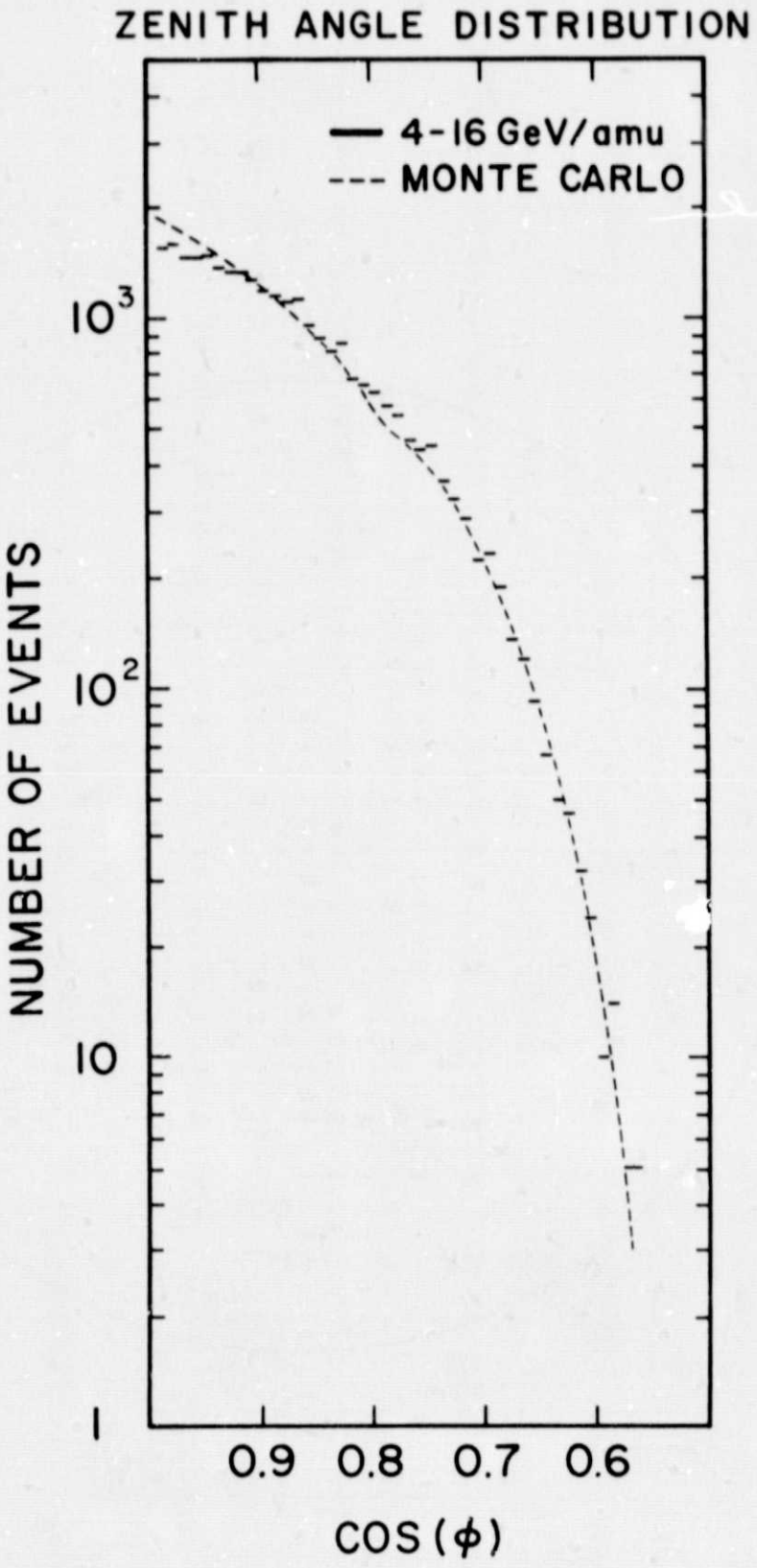
ZENITH ANGLE DISTRIBUTION
4-16 GeV/amu
MONTE CARLO
NUMBER OF EVENTS
10³
10²
10
1
0.9
0.8
0.7
0.6
COS (φ)

TRAJECTORY IMPACT LOCATIONS AT GAS ČERENKOV

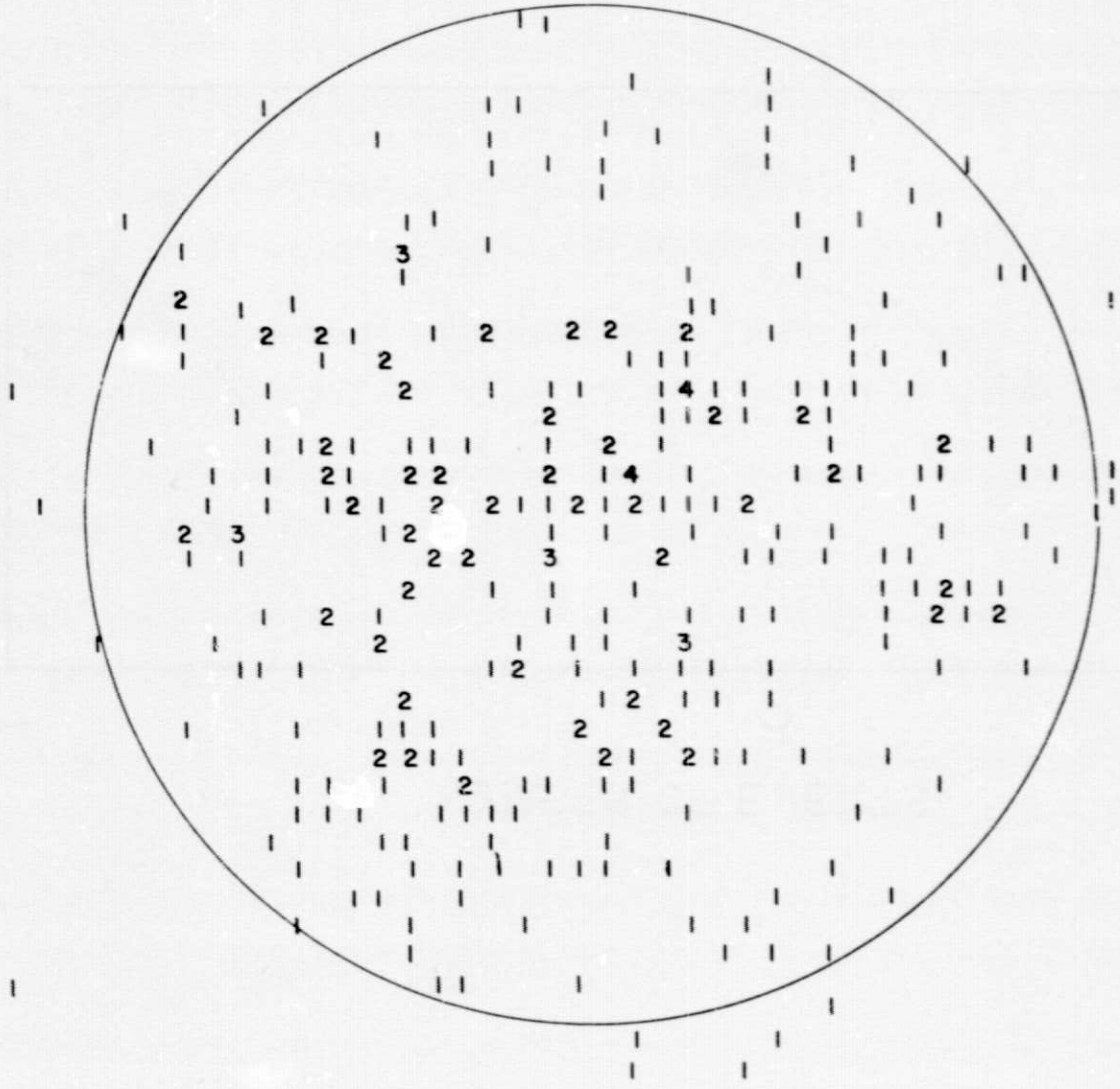

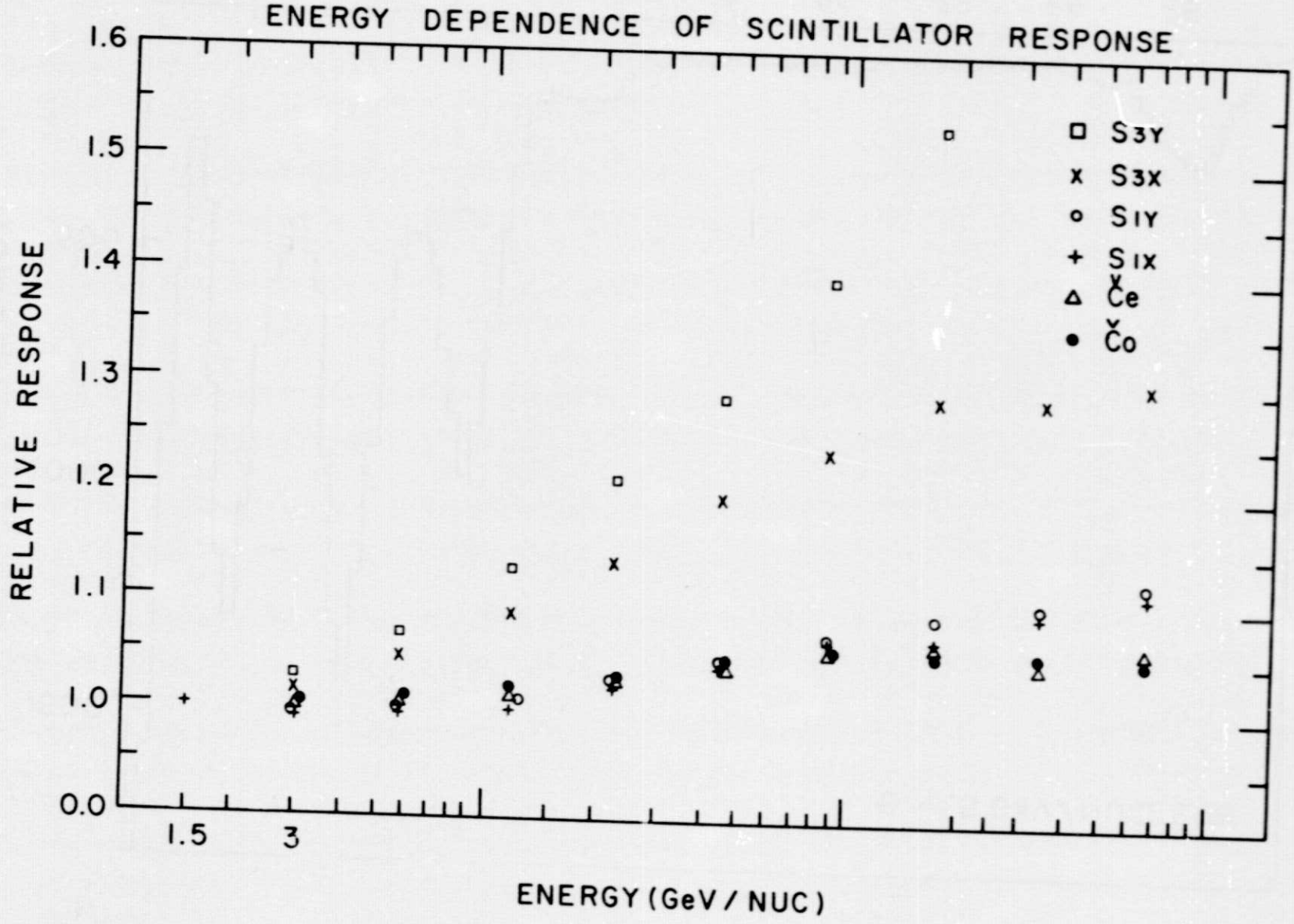
ENERGY DEPENDENCE OF SCINTILLATOR RESPONSE
RELATIVE RESPONSE
1.6
1.5
1.4
1.3
1.2
1.1
1.0
0.0
1.5
3
ENERGY (GeV / NUC)
S3Y
S3X
S1Y
S1X
Ce
Co

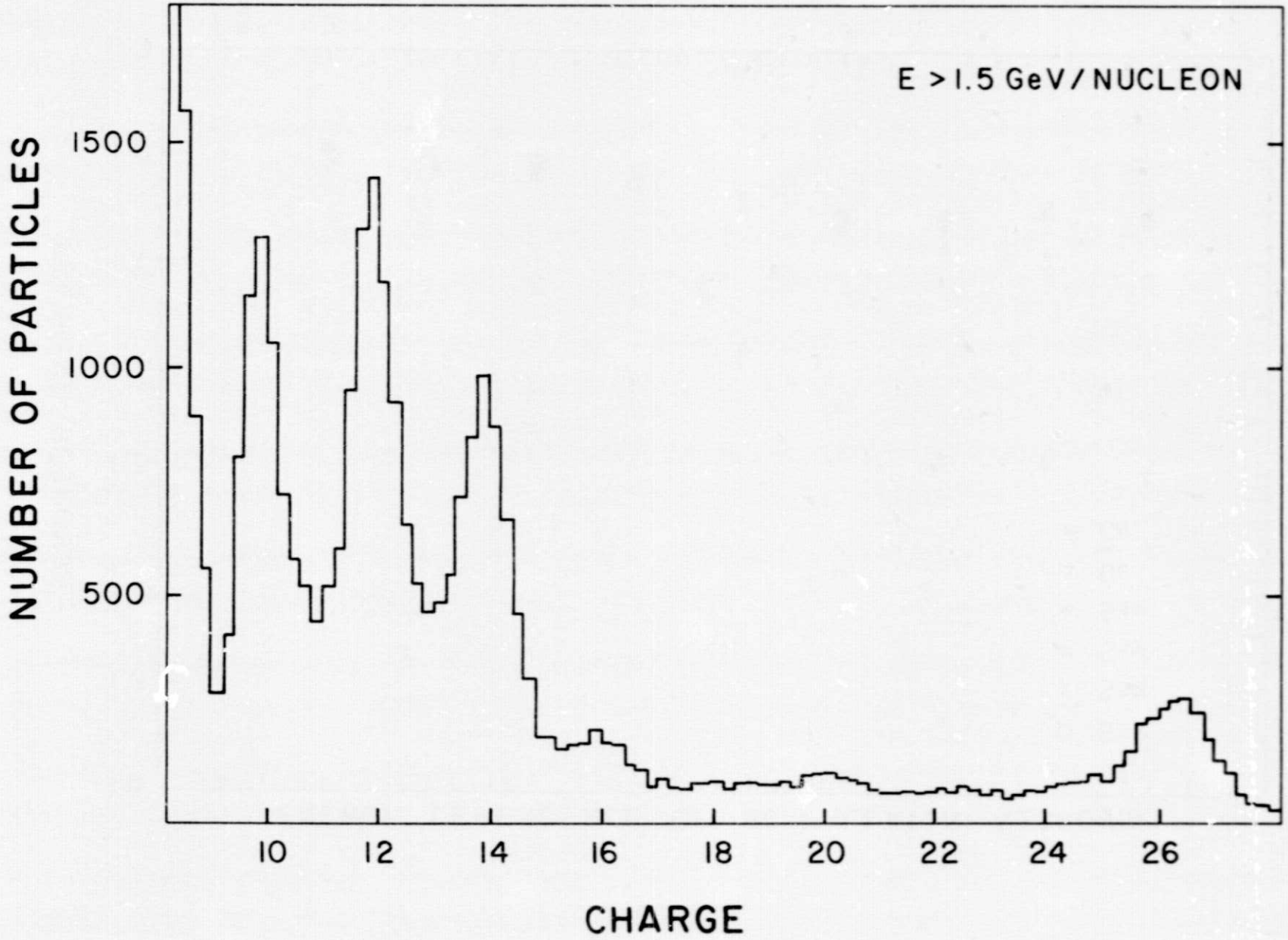
E > 1.5 GeV / NUCLEON
NUMBER OF PARTICLES
1500
1000
500
10
12
14
16
18
20
22
24
26
CHARGE

IONIZATION SPECTROMETER

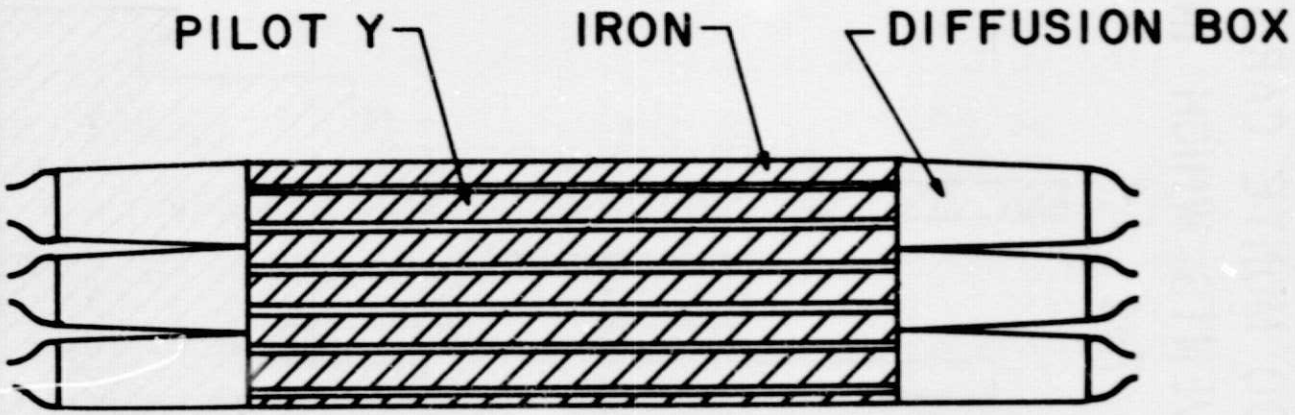

ABSORBER 170 G / CM^2 IRON
+ 5.9 G / CM^2 PILOT Y

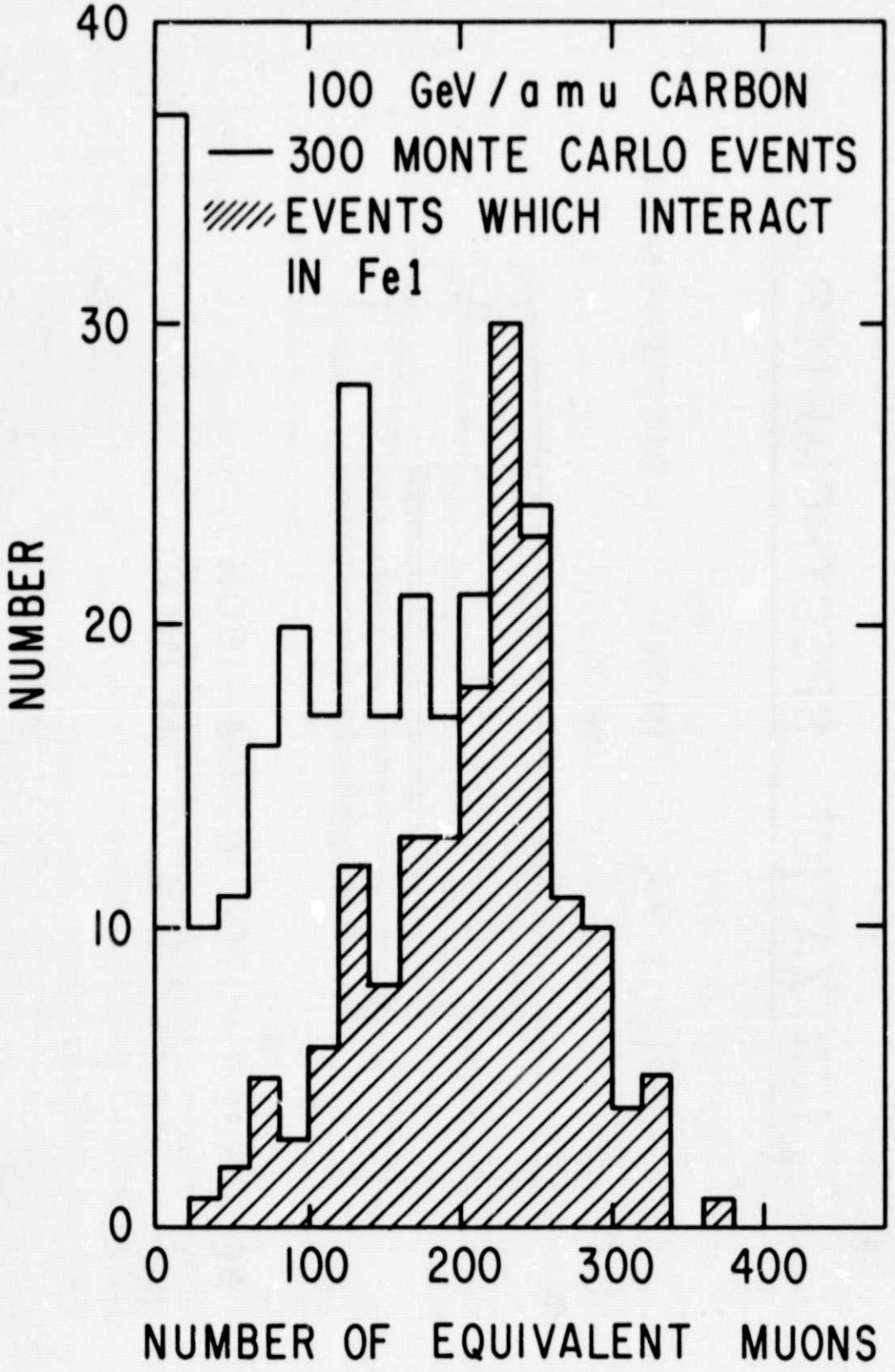
100 GeV / a m u CARBON
300 MONTE CARLO EVENTS
EVENTS WHICH INTERACT
IN Fe1
NUMBER
40
30
20
10
0
0
100
200
300
400
NUMBER OF EQUIVALENT MUONS

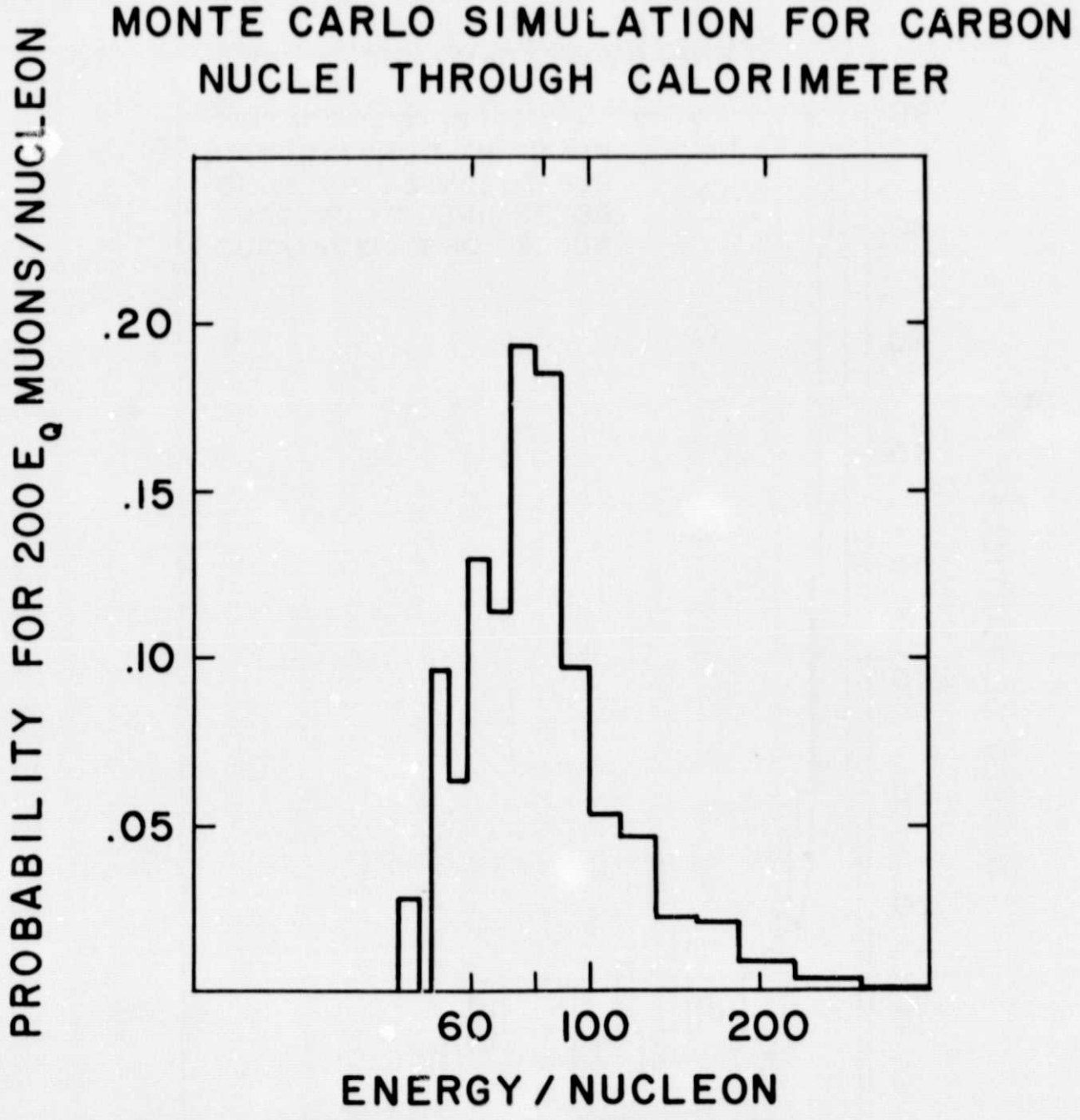
MONTE CARLO SIMULATION FOR CARBON NUCLEI THROUGH CALORIMETER
PROBABILITY FOR 200 E_q MUONS/NUCLEON
.20
.15
.10
.05
60
100
200
ENERGY / NUCLEON

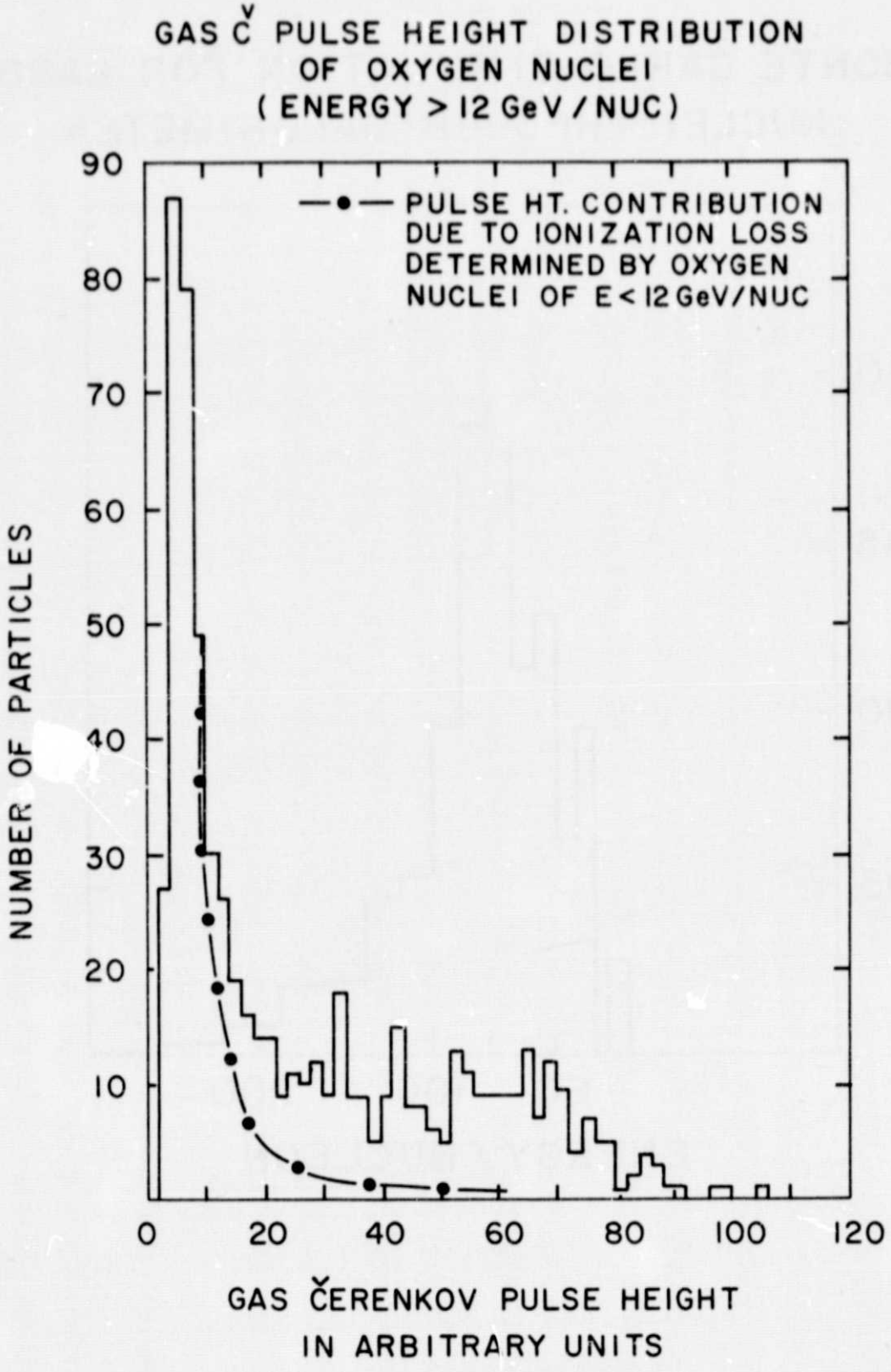
GAS Č PULSE HEIGHT DISTRIBUTION
OF OXYGEN NUCLEI
(ENERGY > 12 GeV / NUC)
PULSE HT. CONTRIBUTION
DUE TO IONIZATION LOSS
DETERMINED BY OXYGEN
NUCLEI OF E < 12 GeV/NUC
NUMBER OF PARTICLES
90
80
70
60
50
40
30
20
10
0
20
40
60
80
100
120
GAS ČERENKOV PULSE HEIGHT
IN ARBITRARY UNITS

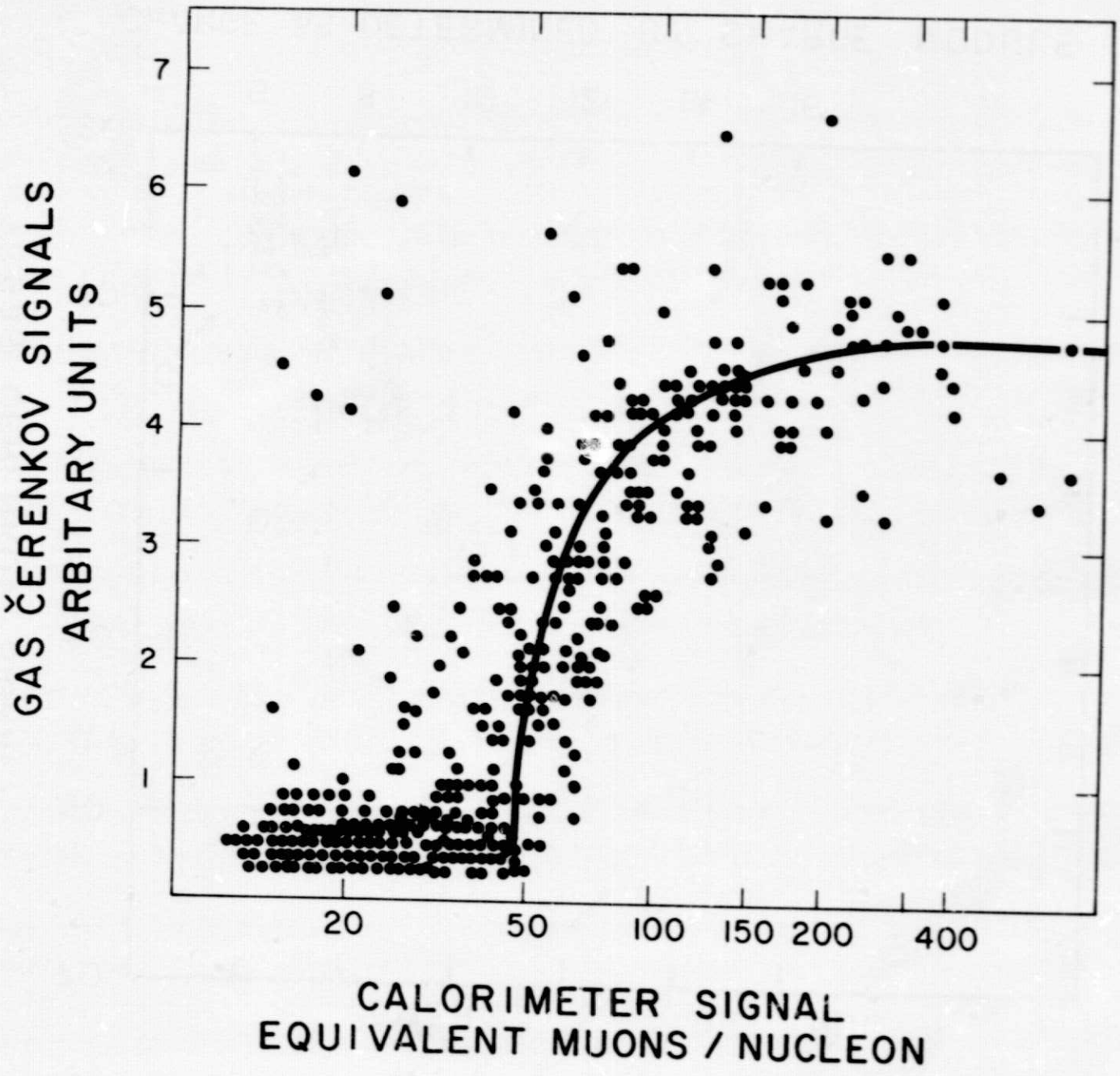
GAS ČERENKOV SIGNALS
ARBITARY UNITS
7
6
5
4
3
2
1
20
50
100
150
200
400
CALORIMETER SIGNAL
EQUIVALENT MUONS / NUCLEON

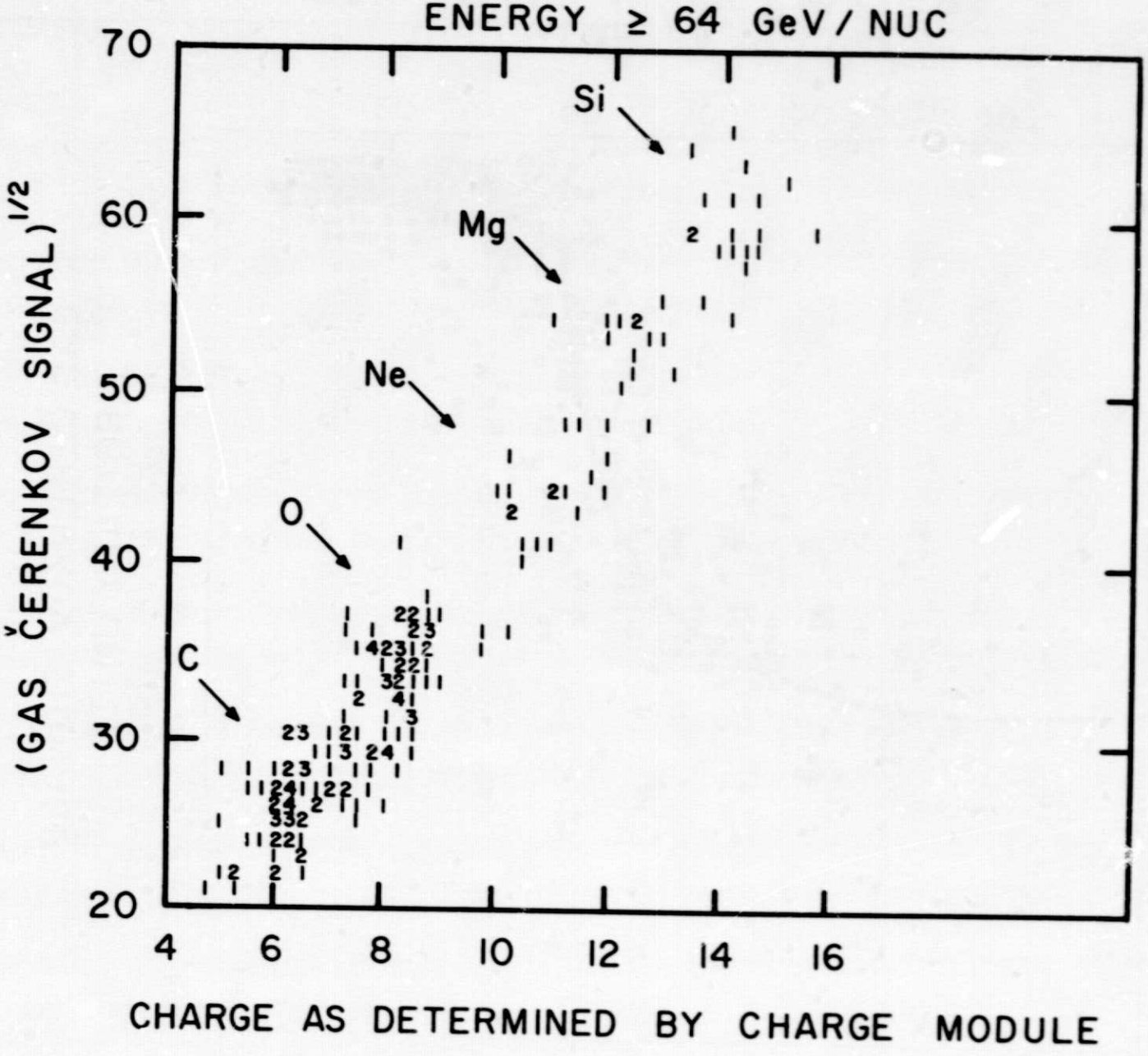
ENERGY ≥ 64 GeV / NUC
(GAS ČERENKOV SIGNAL)^1/2
CHARGE AS DETERMINED BY CHARGE MODULE
Si
Mg
Ne
O
C
70
60
50
40
30
20
4
6
8
10
12
14
16